eLIFE
elifesciences.org

Figures and figure supplements

Sensory experience during locomotion promotes recovery of function in adult visual cortex

Megumi Kaneko, Michael P Stryker

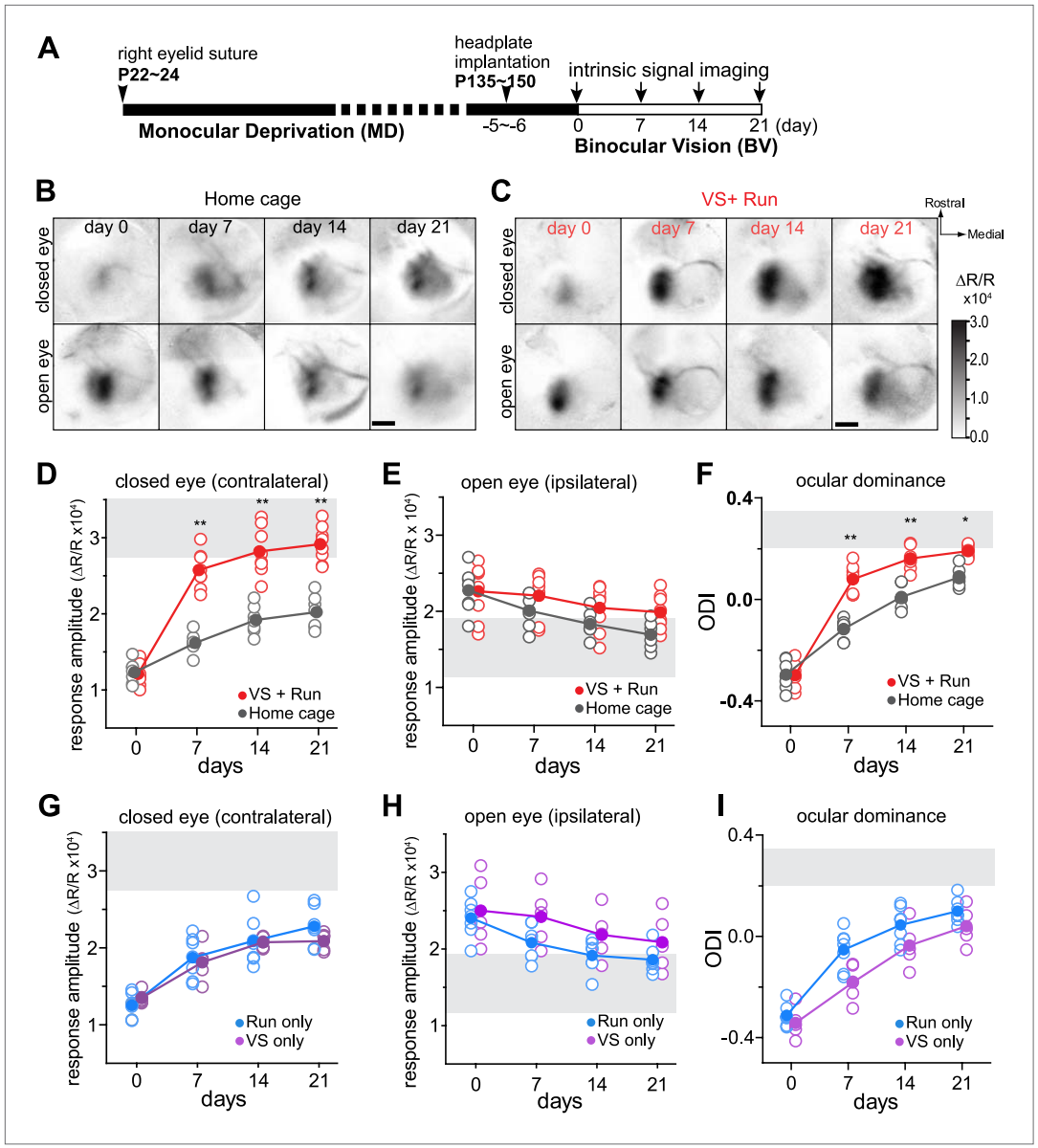

Figure 1. Visual stimulation during locomotion enhances recovery of cortical responses through the deprived eye after prolonged MD. (**A**) Experimental schedule to examine changes in visual cortical responses over 21d-BV following prolonged MD started at postnatal day (P) 22–24. (**B** and **C**) Examples of intrinsic signal responses to the closed eye in the binocular visual cortex during 21d-BV in a *home-cage* control mouse (**B**) and in a mouse viewing contrast-modulated noise as VS during daily runs (*VS+run*, **C**). (**D** and **E**) Changes in intrinsic signal responses evoked by the noise through the closed (**D**) and open (**E**) eyes in *home-cage* (n = 8) and *VS+run* mice (n = 8). (**F**) Ocular dominance index (ODI) computed from response amplitude to contralateral (closed) and ipsilateral (open) eyes shown in **D** and **E**. ODI represents normalized difference in response magnitude between two eyes with 0 being equal amplitude to two eyes; the higher the number, more contralateral eye dominant. (**G** and **H**) Changes in intrinsic signal responses evoked by the noise through the closed (**G**) and open (**H**) eyes in *run-only* (n = 7) and *VS-only* mice (n = 7). (**I**) Ocular dominance index (ODI) computed from response amplitude to contralateral (closed) and ipsilateral (open) eyes shown in **G** and **H**. Gray area in **D**–**I** indicates the range of response amplitude or ODI in age-matched mice with normal visual experience. **p<0.01, *p<0.05, between groups.

DOI: 10.7554/eLife.02798.003

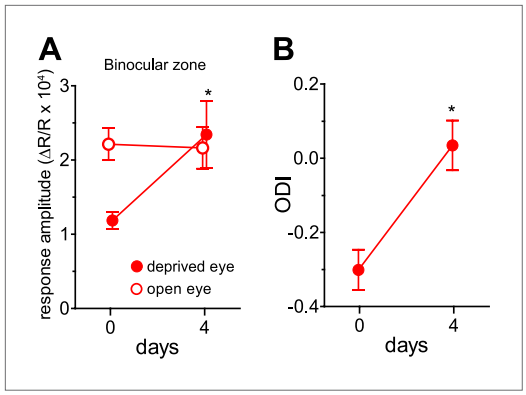

Figure 1—figure supplement 1. Effects of visual stimulation during locomotion after 4 days of binocular vision.

DOI: 10.7554/eLife.02798.004

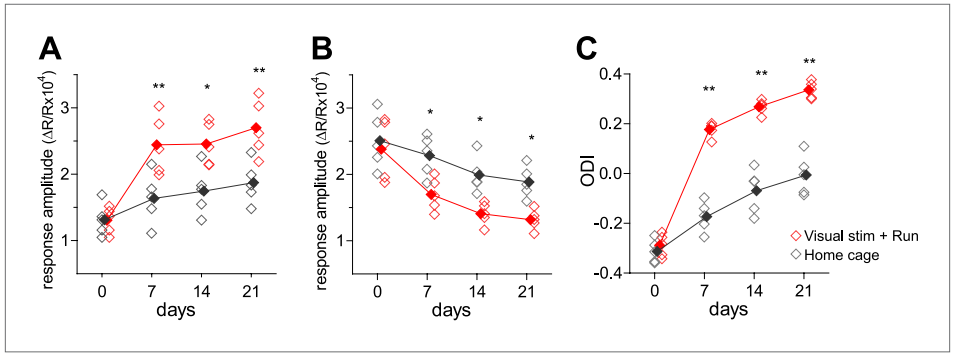

Figure 1—figure supplement 2. Changes in responses during reverse occlusion measured using intrinsic signal imaging.

DOI: 10.7554/eLife.02798.005

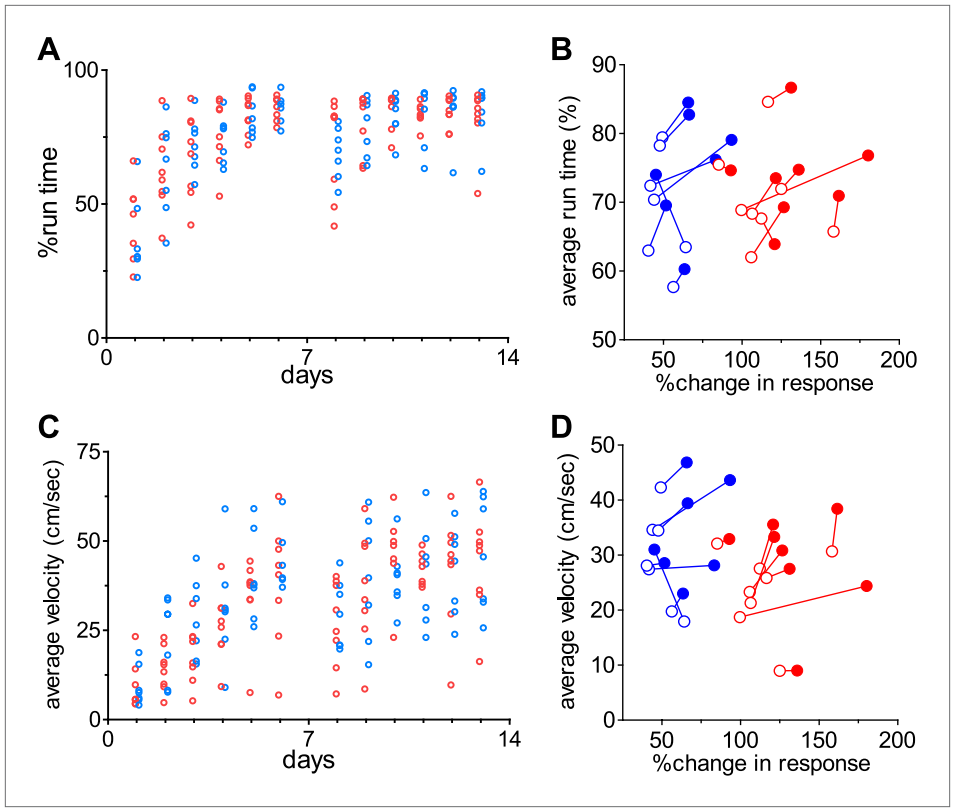

Figure 1—figure supplement 3. Monitoring of locomotion while the mice are on the track-ball.
DOI: 10.7554/eLife.02798.006

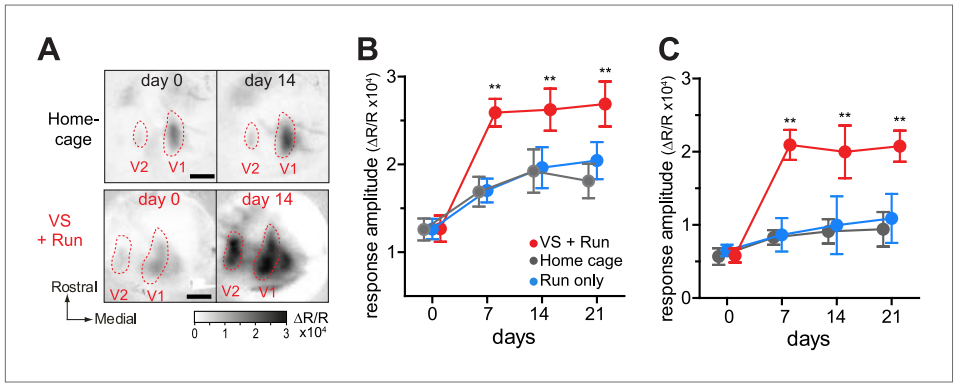

Figure 2. Visual stimulation during locomotion enhances recovery of cortical responses in the monocular visual cortex after prolonged MD. (**A**) Examples of intrinsic signal images of monocular visual areas. (**B** and **C**) Changes in intrinsic signal magnitudes (mean ± SEM) through the closed eye in response to the noise in the monocular V1 (**B**) and monocular secondary visual cortex (**C**) (same animals shown in ***Figure 1D–F***). **p<0.01, between groups.
DOI: 10.7554/eLife.02798.007

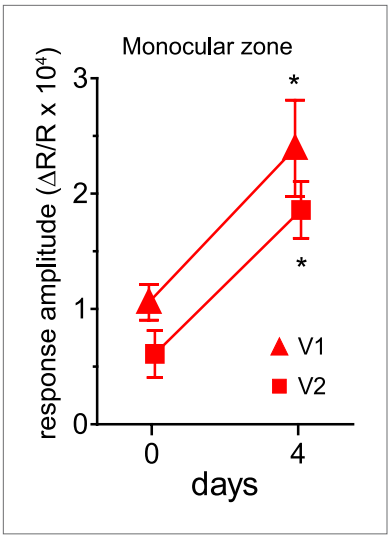

Figure 2—figure supplement 1. Effects of visual stimulation during locomotion on responses in the monocular zone after 4 days of binocular vision.

DOI: 10.7554/eLife.02798.008

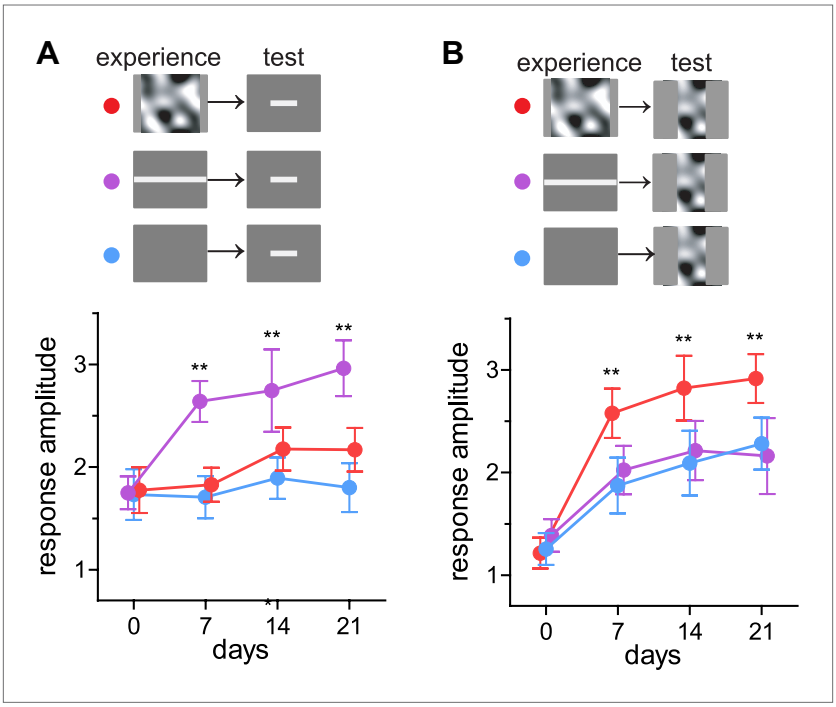

Figure 3. Preferential enhancement of recovery of closed-eye responses to the visual stimuli experienced during locomotion. (**A**) Peak intrinsic signal amplitude in response to bar stimuli through the closed eye in mice that experienced noise (*noiseVS+run*, red, n = 6), drifting bars (*barVS+run*, n = 6), or a blank screen during running (blue, n = 6). (**B**) Peak intrinsic signal amplitude in response to bar stimuli in same mice as in **A**. Data are show mean ± SD. **p<0.01 and *p<0.05 compared with the blank-screen control (blue).

DOI: 10.7554/eLife.02798.009

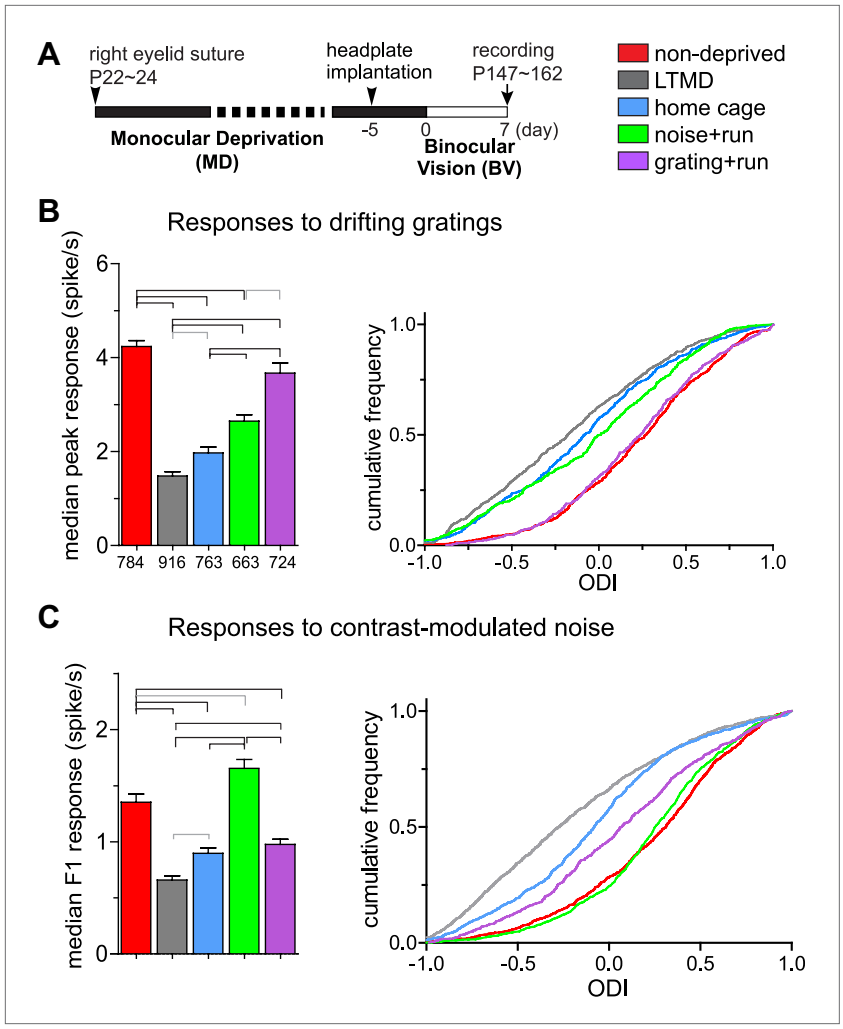

Figure 4. Response magnitude of individual broad-spiking cells to drifting gratings and contrast-modulated noise. (**A**) Experimental schedule for single unit recording. Color-coded bars for different treatment groups apply to all panels. (**B**) Response magnitude to drifting gratings. Left panel: median (±s.e.) response rates to optimal drifting gratings through the deprived eye. Right panel: cumulative frequency distribution of ocular dominance index (ODI) in cells that were responsive (>2 spikes/s) through either deprived or open eye. ODI was computed from response magnitude to optimal gratings through each eye as shown in ***Figure 4—figure supplement 1A***. (**C**) Response magnitude to contrast-modulated noise. Left: median F1 response (±s.e.) to the noise stimulus through the deprived eye. Right: cumulative frequency distribution of ODI calculated for each cell that were responsive to the noise (F1 response >0.2) through either eye from the data shown in ***Figure 4—figure supplement 1B***. Data in left panels of **B** and **C** are from same populations of all cells isolated, as numbers are indicated below bars in **B**. Horizontal lines above bars; black: $p<0.01$, gray: $p<0.05$. Results of Kolmogorov–Smirnov tests for cumulative frequency distributions are shown in ***Table 1***.

DOI: 10.7554/eLife.02798.010

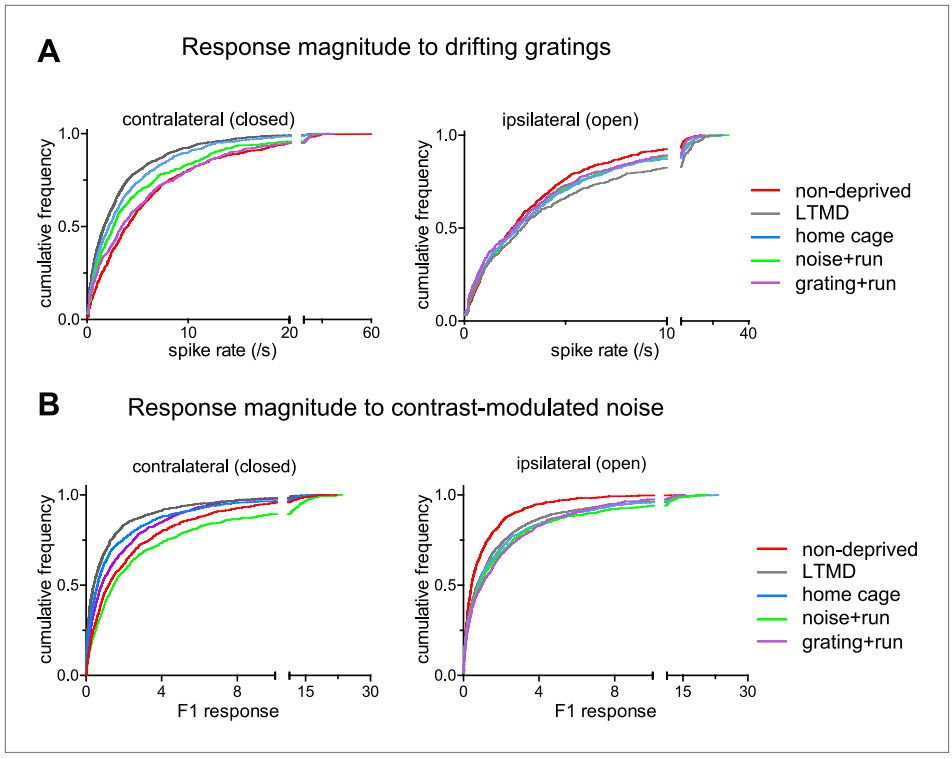

Figure 4—figure supplement 1. Response magnitudes of individual broad-spiking cells to drifting gratings and contrast-modulated noise.

DOI: 10.7554/eLife.02798.011

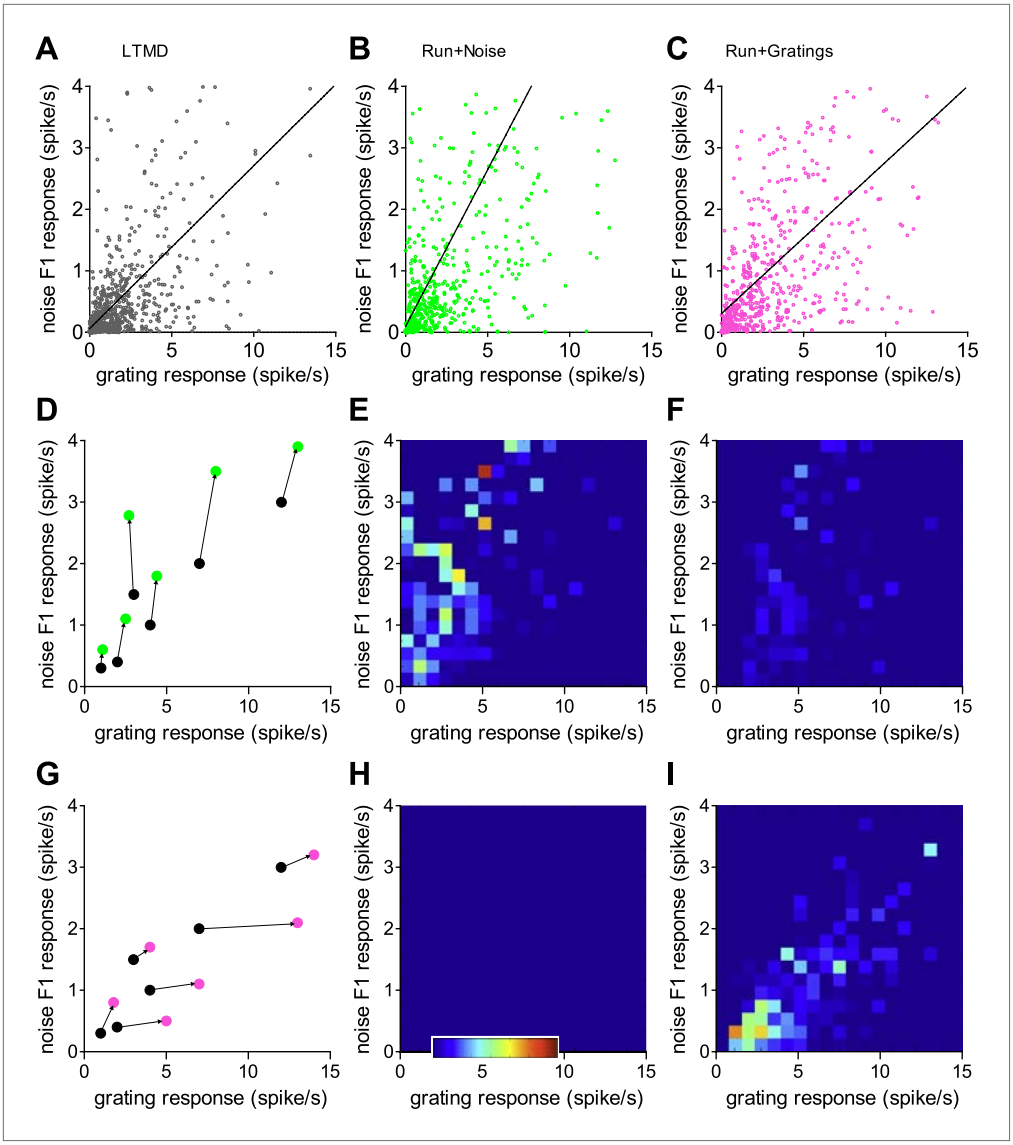

Figure 4—figure supplement 2. Analysis of fictive longitudinal data on the stimulus specificity of recovery during locomotion.

DOI: 10.7554/eLife.02798.012

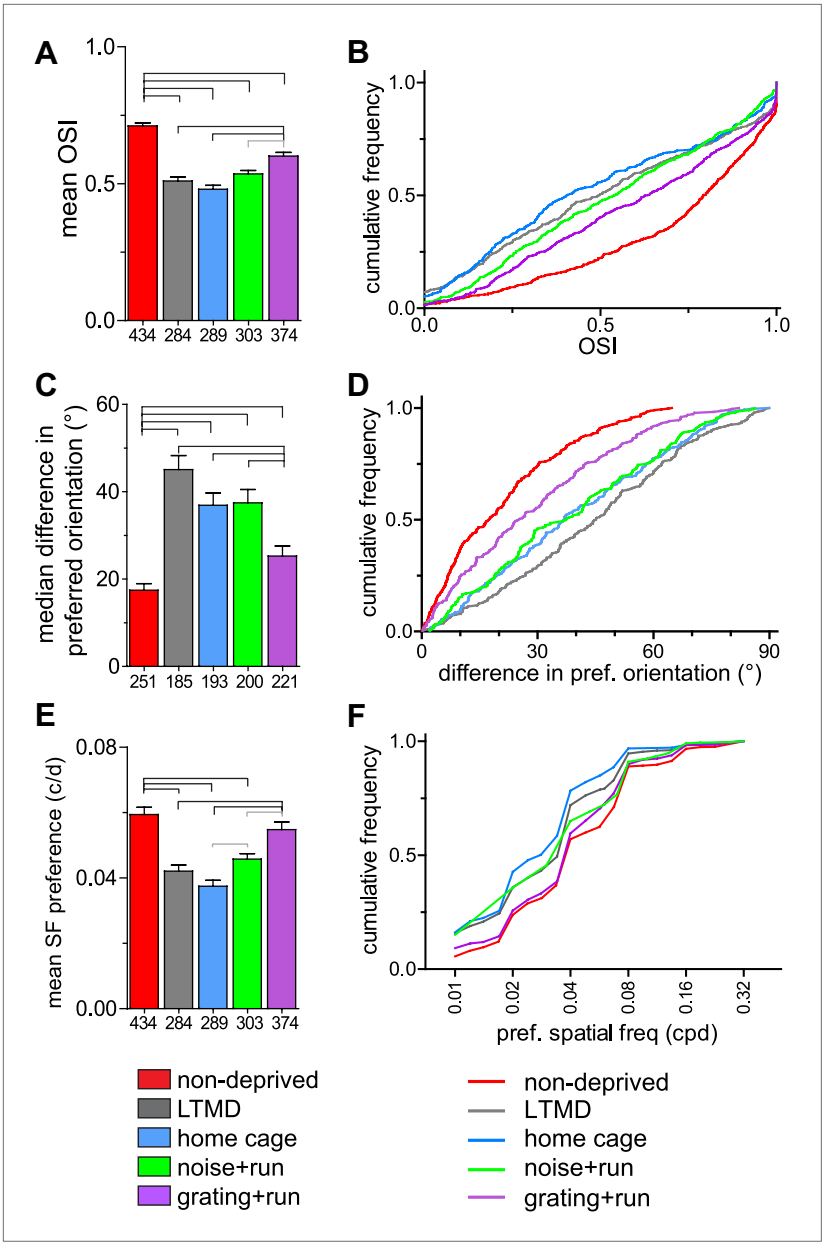

Figure 5. Tuning properties of individual broad-spiking cells in response to drifting gratings. (**A** and **B**) Orientation tuning of deprived-eye responses, expressed as mean (±SEM) orientation selectivity index (OSI) (**A**) and cumulative frequency distribution of OSI (**B**). (**C** and **D**) Binocular matching of preferred orientation. Absolute differences in preferred orientation between two eyes in binocularly responsive cells are presented as the median (±s.e.) (**C**) and the cumulative frequency distribution (**D**). (**E** and **F**) Spatial frequency tuning. Preferred spatial frequencies at the preferred orientation of drifting gratings through the deprived eye are shown as mean (±SEM) (**E**) and cumulative frequency distribution (**F**). Sample sizes are indicated below bars. Horizontal lines above bars; black: $p<0.01$, gray: $p<0.05$. Results of Kolmogorov–Smirnov tests for **B**, **D**, **F** are shown in ***Table 1***.

DOI: 10.7554/eLife.02798.017

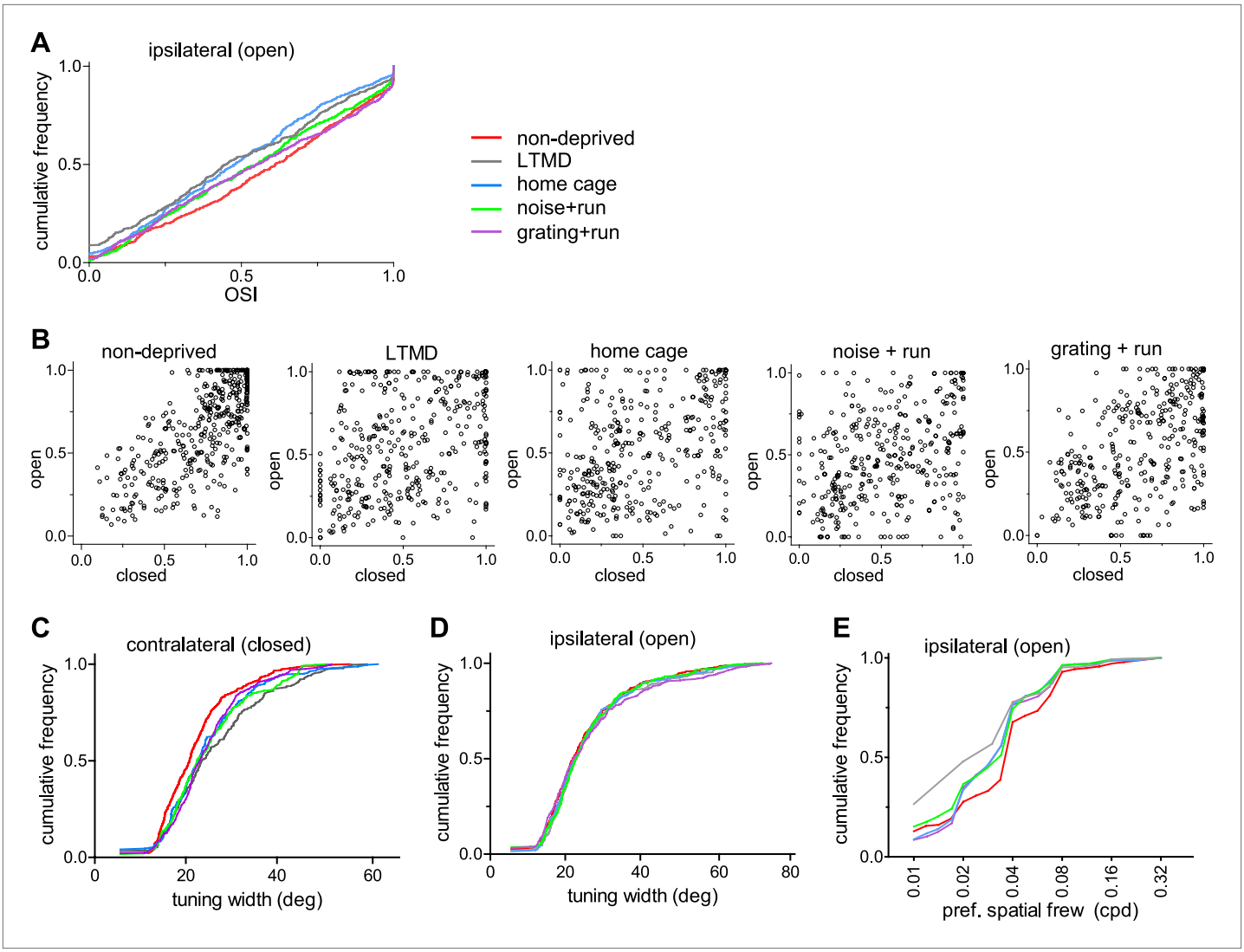

Figure 5—figure supplement 1. Tuning properties of broad-spiking cells examined with drifting sinusoidal gratings.

DOI: 10.7554/eLife.02798.018

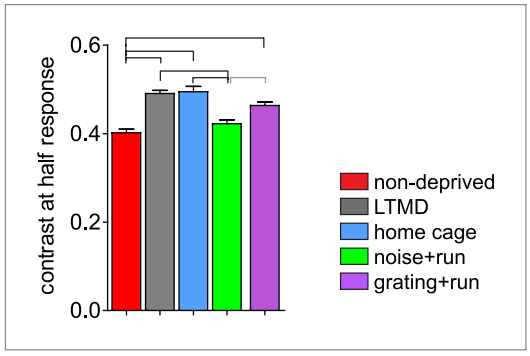

Figure 6. Change in contrast sensitivity in broad-spiking cells. Average values of contrast that gives half-maximal response are shown. Horizontal lines above bars; black: $p<0.01$, grey: $p<0.05$.

DOI: 10.7554/eLife.02798.019

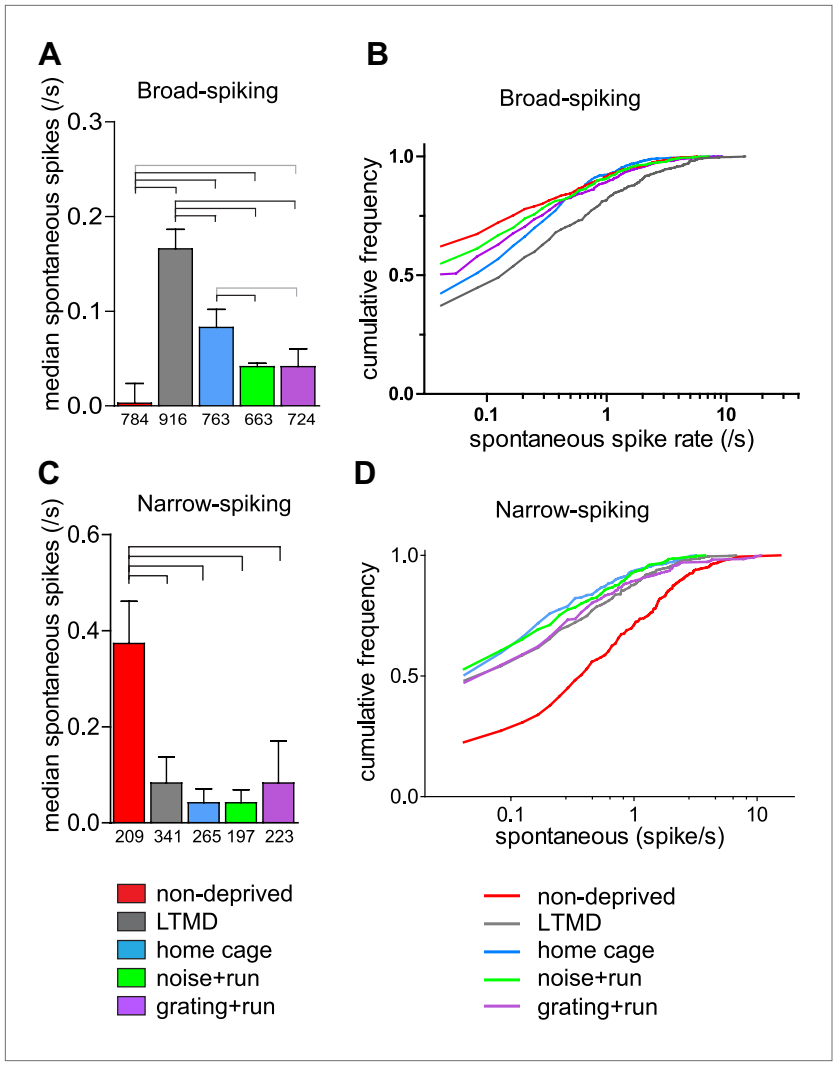

Figure 7. Spontaneous firing of isolated broad-spiking and narrow-spiking cells recorded simultaneously. (**A** and **B**) The median (±s.e.) number (**A**) and cumulative frequency distribution (**B**) of spontaneous firing rates of all broad-spiking cells isolated during the presentation of blank screen randomly interspaced in the drifting grating set. (**C** and **D**) The median (±s.e.) number (**C**) and cumulative frequency distribution of spontaneous firing rates of all narrow-spiking cells. Sample sizes are indicated in **A** and **C**. Horizontal lines above bars; black: $p<0.01$, grey: $p<0.05$. Results of Kolmogorov–Smirnov tests for **B** and **D** are shown in ***Table 1***.

DOI: 10.7554/eLife.02798.020

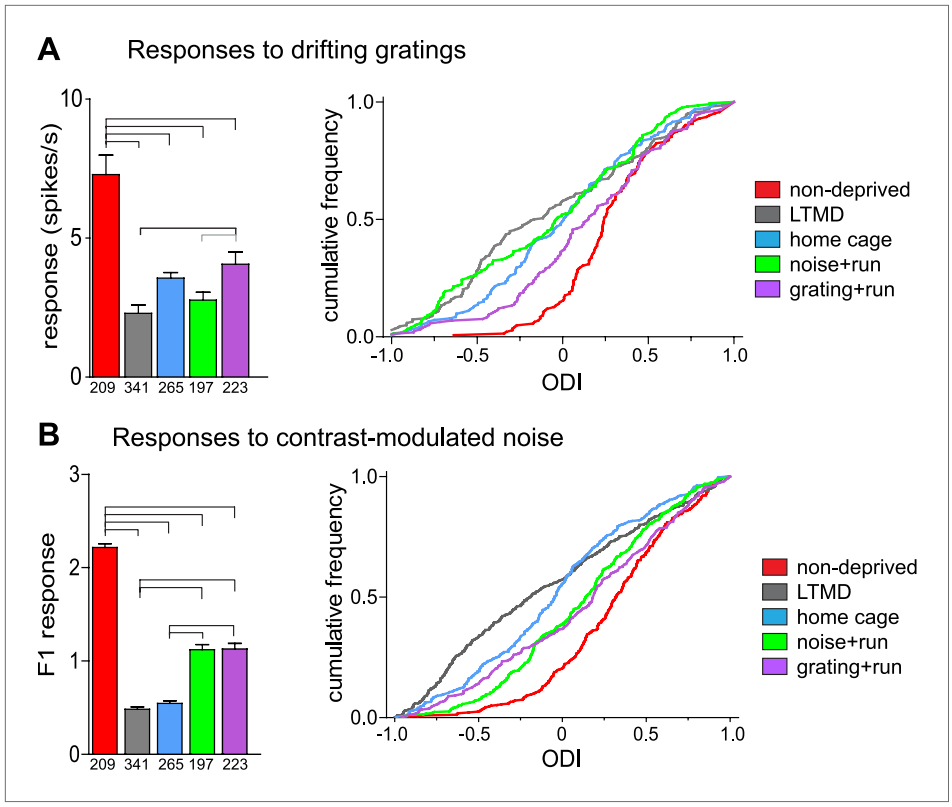

Figure 8. Responses of isolated narrow-spiking cells recorded simultaneously with broad-spiking cells. (**A**) Responses to drifting sinusoidal gratings of all narrow-spiking cells isolated. Left: median ±s.e. of peak responses to the optimal gratings through the deprived eye. Right: cumulative frequency distribution of ocular dominance index (ODI) calculated for each cell from peak responses through the deprived eye (as shown in ***Figure 8—figure supplement 1A***) and the open eye (***Figure 8—figure supplement 1B***). (**B**) Responses to contrast-modulated noise in all narrow-spiking cells isolated. Left: median ±s.e. of F1 responses through the deprived eye. Right: cumulative frequency distribution of ocular dominance index (ODI) calculated for each cell from F1 responses through the deprived eye (as shown in ***Figure 8—figure supplement 1C***) and the open eye (***Figure 8—figure supplement 1D***). Horizontal lines above bars; black: $p<0.01$, grey: $p<0.05$. Results of Kolmogorov–Smirnov tests for cumulative frequency distributions are shown in ***Table 1***.

DOI: 10.7554/eLife.02798.021

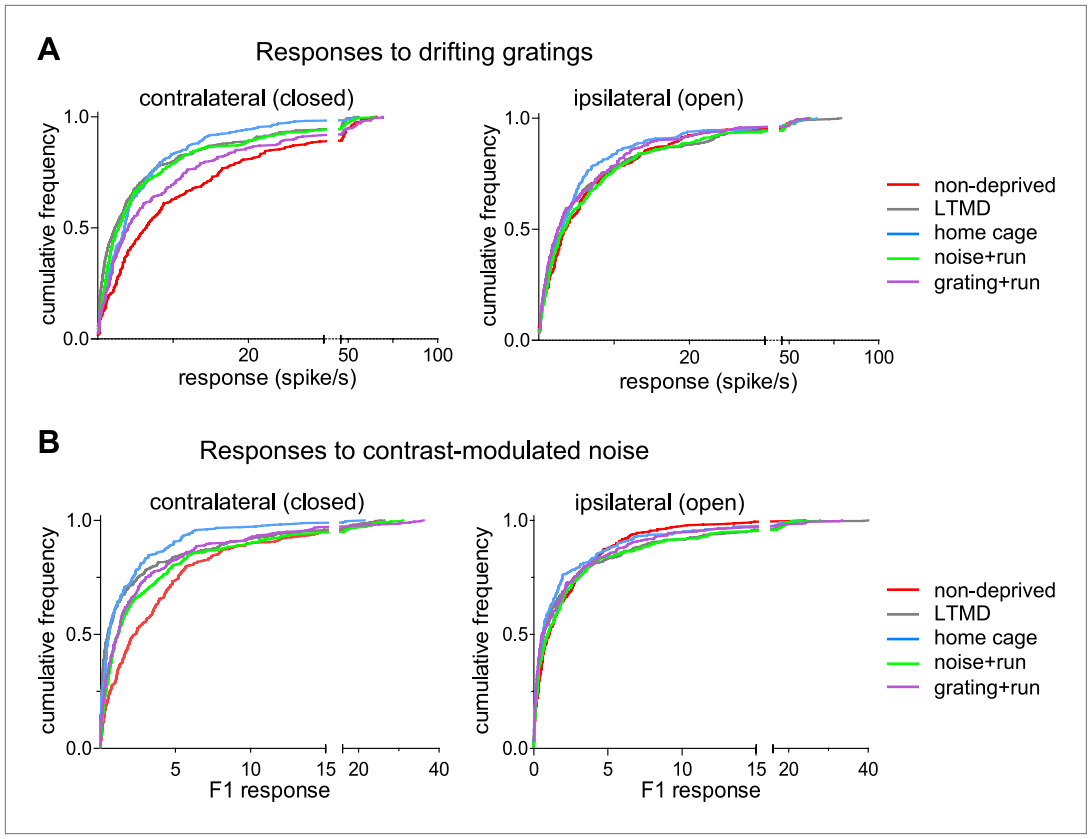

Figure 8—figure supplement 1. Responses of isolated narrow-spiking cells recorded simultaneously with broad-spiking cells.

DOI: 10.7554/eLife.02798.022